Published in final edited form as:
Int J Radiat Biol. 2014 September ; 90(9): 821–830. doi:10.3109/09553002.2014.927935.

Total-Body Irradiation Produces Late Degenerative Joint Damage in Rats

Ian D. Hutchinson[1], **John Olson**[2], **Carl A. Lindburg**[3], **Valerie Payne**[3,4], **Boyce Collins**[5], **Thomas L. Smith**[1], **Michael T. Munley**[3,4], **Kenneth T. Wheeler**[2,4], and **Jeffrey S. Willey**[1,3,4]

[1]Department of Orthopaedic Surgery, Wake Forest School of Medicine, Winston-Salem, NC

[2]Department of Radiology, Wake Forest School of Medicine, Winston-Salem, NC

[3]Department of Radiation Oncology, Wake Forest School of Medicine, Winston-Salem, NC

[4]Comprehensive Cancer Center, Wake Forest School of Medicine, Winston-Salem, NC

[5]Engineering Research Center for Revolutionizing Metallic Biomaterials, North Carolina A&T, Greensboro, NC

Abstract

Purpose—Premature musculoskeletal joint failure is a major source of morbidity among childhood cancer survivors. Radiation effects on synovial joint tissues of the skeleton are poorly understood. Our goal was to assess long-term changes in the knee joint from skeletally mature rats that received total-body irradiation while skeletal growth was ongoing.

Materials and Methods—14 week-old rats were irradiated with 1, 3 or 7 Gy total-body doses of 18 MV x-rays. At 53 weeks of age, structural and compositional changes in knee joint tissues (articular cartilage, subchondral bone, and trabecular bone) were characterized using 7T MRI, nanocomputed tomography (nanoCT), microcomputed tomography (microCT), and histology.

Results—T2 relaxation times of the articular cartilage were lower after exposure to all doses. Likewise, calcifications were observed in the articular cartilage. Trabecular bone microarchitecture was compromised in the tibial metaphysis at 7 Gy. Mild to moderate cartilage erosion was scored in the 3 and 7 Gy rats.

Conclusions—Late degenerative changes in articular cartilage and bone were observed after total body irradiation in adult rats exposed prior to skeletal maturity. 7T MRI, microCT, nanoCT, and histology identified potential prognostic indicators of late radiation-induced joint damage.

Keywords

Radiation; articular cartilage; knee joints; arthritis; 7T MRI; nanocomputed tomography

Corresponding Author: Jeffrey S. Willey, Wake Forest School of Medicine, 411 NRC, Radiation Biology Section, Medical Center Blvd, Winston-Salem, NC 27157. Phone: 336-713-7637. jwilley@wakehealth.edu.

Declaration of Interest Statement: The authors report no declarations of interest

Introduction

Ionizing radiation is used to treat childhood malignancies and pre-condition patients for bone marrow transplantation (Kobos et al. 2012). However, many of these regimens expose unaffected musculoskeletal tissues to potentially damaging levels of radiation (Armenian et al. 2011; Rueegg et al. 2013). The current focus in pediatric patients has first been to successfully treat the presenting condition and then manage the systemic co-morbidities associated with radiation therapy, including endocrine, neurological, gastrointestinal, respiratory, and reproductive dysfunction and secondary malignancies (Bhatia & Sklar 2002; Faraci et al. 2005; Oeffinger & Bhatia 2009; Greene-Schloesser et al. 2012). In the musculoskeletal system, the clinical concerns in children have been altered growth, bone fracture, spinal deformity, osteochondroma, and secondary bone malignancies (Leiper et al. 1987; Chemaitilly et al. 2007; Shido et al. 2012). Metaphyseal trabecular bone changes, osteonecrosis of the femoral head, growth plate cartilage manifestations, including slipped capital femoral epiphysis, and platyspondylyl of the spine have been well studied and documented (Kaste et al. 2004; Damron et al. 2008; Damron et al. 2009; Miyazaki et al. 2009; Pritchard et al. 2010; Mostoufi-Moab et al. 2012; Mostoufi-Moab et al. 2013).

Although chronic musculoskeletal health has not been an immediate concern of the treating physicians and translational researchers, decreased mobility and premature joint failure have recently emerged as major sources of morbidity among childhood cancer survivors (Hudson et al. 2003; Oeffinger et al. 2006; Braam et al. 2013). For example, Oeffinger et al. (2006) found an adjusted relative risk of 54 for joint replacement in pediatric cancer survivors when compared to age-matched sibling controls with a mean age of 26.6 years. In this cohort, 62.2% of the patients received radiation therapy. The development of debilitating degenerative joint damage may account in part for the decreased mobility observed in childhood cancer survivors; decreased mobility has negative psychosocial consequences directly impacting quality of life and likely influencing mental health outcomes (Hudson et al. 2003; Braam et al. 2013). Decreased mobility also impacts cardiovascular and respiratory health (Oeffinger et al. 2006).

Following childhood exposure to pre-conditioning total-body irradiation (TBI) for bone marrow transplantation, Miyazaki et al. (2009) describe a series of early bone changes, including osteochondromata, irregular epiphyseal ossification, metaphyseal fraying, striations and sclerosis, osteochondromas, slipped femoral epiphysis, genu valgum and platyspondylyl. Nine of the eleven patients in their study had painful or unstable hip and/or knee joints (Miyazaki et al. 2009). Indeed, the finding of painful symptomatic valgus knee joints following irradiation has been described elsewhere (King et al. 2013; Fletcher et al. 1994). However, current clinical studies fail to follow progressive, debilitating articular cartilage degenerative changes in children and adolescents after irradiation out to early adulthood where their risk of joint replacement is significant. Moreover, the link between radiation-induced articular cartilage damage and joint failure has been tenuously made following occupational and therapeutic radiation exposure in adults, not children (Kolar et al. 1967; Collis et al. 1988).

The effects of radiation on articular cartilage remain poorly understood. Radiation exposure has been shown to cause acute degenerative alterations of the cartilage matrix composition and metabolism *in vitro*; specifically, radiation is known to lower proteoglycan (PGs) content and compressive stiffness (Cornelissen & de Ridder 1990; Cornelissen et al. 1993, 1996; Pritchard et al. 2010; Lindburg et al. 2013; Willey et al. 2013). Biological changes in the joint are also likely influenced by radiation-induced bone changes and biomechanical alterations across the joint that disrupt the normal distribution of forces. Osteonecrosis that alters the shape of the femoral head and the nature of the articulation can cause secondary osteoarthritis in the hip by modifying cartilage loading (Bullough & DiCarlo 1990). In the context of whole joint health, potential radiation-induced changes to the stabilizing ligaments, menisci, and muscles may further alter joint knee kinematics as well as contribute to a catabolic milieu within the joint (Stone et al. 2014). It is important to consider that the clinical evidence suggests an indolent pathological process in irradiated childhood cancer survivors with the increased incidence of premature joint failure and replacement only becoming evident at long term follow-up (Oeffinger et al. 2006).

The use of advanced imaging technologies to identify and evaluate bone and joint disorders in preclinical animal models is gaining popularity (Tremoleda et al. 2011). Quantitative Magnetic Resonance Imaging (qMRI) has been applied both in animals and humans in an attempt to understand the pre-clinical window of joint degeneration by identifying morphological and compositional changes in cartilage that precede clinical symptoms (Andreisek & Weiger 2014).

Alterations in whole joint homeostasis, cartilage biology, and biomechanics have been shown to result in early changes in composition of the articular cartilage and the underlying subchondral bone in osteoarthritis (Lammentausta et al. 2006; Loeser et al. 2012; Kazakia et al. 2013; Andreisek & Weiger 2014). The T2 relaxation time is emerging as a biomarker of articular cartilage status because it can quantitatively measure the, i] loss of collagen fiber orientation and integrity, and ii] glycosaminoglycan content. Both are associated with changes in bound water, a characteristic of early osteoarthritis (Prasad et al. 2013; Wong et al. 2013). In addition, nanofocus computed tomography (nanoCT) is being used to characterize cartilage subtissue architecture. NanoCT has the added advantage of being able to identify and quantitate discrete bony abnormalities and chondrocalcinosis in small animal models (Kerckhofs et al. 2013).

Currently, an *in vivo* model to investigate the late effects of TBI on musculoskeletal joint health in growing individuals is lacking. Such a model is required to investigate the mechanism(s) of radiation-induced premature joint degeneration. Characterizing the clinically quiescent interval between radiation exposure and symptom emergence should identify targets for the development of therapeutic strategies to improve patient outcome. Therefore, the overall goal of our present study was to develop and characterize a rodent model of joint degradation after radiation therapy during skeletal development.. The development of this model requires the use of, i] clinically relevant radiation doses, ii] advanced radiological imaging techniques capable of detecting preclinical compositional soft tissue changes, and iii] validated protocols that characterize musculoskeletal damage in rodents, including quantitative measures of radiation induced trabecular bone degradation

and histological measures of articular cartilage degeneration. The methods and rat model described below should enable radiation-induced joint damage to be characterized immediately after radiation exposure and longitudinally during progression of the damage.

Materials and Methods

Animal model

Sixteen adolescent male Fisher F344 X Brown Norway rats were purchased (Harlan Laboratories, Dublin, VA, USA) at 12 weeks of age and housed in pairs on a 12 h light/dark cycle with food and water *ad libitum*. All experiments and animal handling were performed in strict accordance with the NIH Guide for Care and Use of Laboratory Animals as approved by the Wake Forest School of Medicine Institutional Animal Care and Use Committee.

The irradiation treatments and sham-irradiations were performed on these rats following a 2 week acclimation period when the rats were 14 weeks of age. At an age of 14 weeks, the stage of musculoskeletal maturity in rats is approximates a 9 year-old human (Quinn 2005). Thus treatments were performed while skeletal growth was still ongoing. Tissues were collected for analysis when the rats were 53 weeks of age, when the stage of musculoskeletal maturity approximates a skeletally-mature 35 year-old human,(Quinn 2005). It is important to note that rats do not exhibit growth plate closure as do humans (Quinn 2005) and the rate of skeletal growth in 14 week-old rats is much lower than a rat half this age (Hansson et al. 1972), thus some limitations must be placed on the direct comparison between musculoskeletal maturity in rodents and humans.

Irradiation procedure

At 14 weeks of age, 3 groups (n = 4 per group) of these unanesthetized rats were placed in environmental chambers and irradiated with 1, 3 or 7 Gy total-body doses of 18 MV x-rays from a medical linear accelerator at a dose rate of ∼425 mGy/min. The irradiation chambers, setup, and dosimetry were identical to that describe by Walb et al. (2012) for their air-breathing mouse carcinogenesis studies (Walb et al. 2012). Total-body irradiation was performed as childhood leukemia patients receive total-body irradiation as preconditioning for stem cell transplantation. The unirradiated control rats (n = 4) were handled identically to the irradiated rats.

Limb collection

Nine months after irradiation, the rats were euthanized at 53 weeks of age using CO_2 anesthesia followed by decapitation. The right hind limb was removed from the rats, taking care to keep the femur and tibia fully articulated. The tibia and femur were cleaned of soft tissue, fixed for 72 h in 10% neutral buffered formalin, and placed in 70% ethanol until imaged with microCT (n = 4/group), qMRI (n = 4/group), nanoCT (n = 3/group) and then used for histological analyses (n = 3/group). The same hind limb was used for each analysis

Magnetic Resonance Imaging

Image Acquisition—All imaging was performed on the Wake Forest School of Medicine's Bruker Biospec 70/30 horizontal bore 7T MRI (Bruker Biospin, Ettlingen, Germany). The magnet was equipped with a high performance gradient/shim insert capable of producing maximum magnetic field gradients of 1000 mT/m. Magnetic Resonance signal transmission and reception was performed with a 35 mm inside diameter quadrature radio frequency (RF) volume coil. Each rat knee was positioned at the isocenter of both the RF coil and the magnet. A Rapid Acquisition with Relaxation Enhancement (RARE) spin echo pulse sequence was used to acquire a 3 plane scout scan to verify that the center of the knee joint was at the center of the magnet. The 3 plane scout scan parameters were: field of view (FOV) = 4 cm, slice thickness (thk) = 2 mm, repetition time (TR) = 1500 ms, echo time (TE) = 36 ms, matrix size = 256 × 256, number of excitations (NEX) = 1. When the knee was correctly positioned, axial and coronal scout scans were acquired using a RARE pulse sequence with parameters: FOV = 3 cm, thk = 1 mm, TR = 2500 ms, TE = 25 ms, matrix = 128, and NEX = 2. The axial and coronal scout scans were used to plan the sagittal slice placement of the high resolution T2 map sequence. A Multi Slice Multi Echo (MSME) spin echo pulse sequence was used to acquire the T2 relaxometry data. MSME T2 mapping parameters were: FOV = 2 cm, thk = 0.2 mm, Matrix = 512 × 512 (in plane resolution = 39 um), TR = 2000 ms, eight echoes with TE's = 8.5, 17, 25.5, 34, 42.5, 51, 59.5, and 68 ms, and NEX = 72 (Raya et al. 2010).

T2 relaxation time measurement—ImageJ (http://imagej.nih.gov/ij/) was used to manually select regions of interest (ROIs). ROIs were carefully selected with the cartilage-cartilage contact areas in the medial and lateral knee compartments (Figure 1). On the tibial plateau, this constituted the central area not covered by the meniscus using a sagittal slice that lay halfway between the tibial spine and the outer edge of the meniscus. Identifying the standing cartilage-cartilage contact area on the femoral condyle is more difficult in the rat than in the human because it is a function of the resting knee flexion which potentially introduces variability (Walker et al. 2006). Nevertheless, we selected a sagittal slice in the center of the condyle using an ROI of similar size to the tibial plateau, taking care to reduce partial volume effects due the curved topography and minimizing the magic angle effect. The magic angle effect is an artificial shortening of T2 relaxation due to greater than 54.7° discordance of collagen fiber orientation to the magnetic field of the scanner (B_0) as it relates to water mobility (Henkelman et al. 1994; Recht et al. 2005). In the small animal model, erroneous measure of cartilage T2 relaxation due to the magic angle effect may be minimized by considered positioning of the specimen in the scanner and appreciation for the relatively exaggerated topography of the articular surfaces. The mean signal intensity of the voxels in the ROI was measured for each of the 8 acquired echo images. The signal intensities vs echo times were plotted in Excel and fit to a noise corrected exponential decay curve using the equation: $SI^2 = (SIo\ e^{-TE/T2})^2 + (N)^2$ (Figure 1).

MicroCT

The trabecular architecture within the proximal tibial metaphysis of the right hind limb was evaluated using microCT (microCT 80, Scanco Medical AG; Bassersdorf, Switzerland), with isotropic voxels of 18 m/side, at 70 kV and an intensity of 114 μA. An ∼3 mm section

of secondary spongiosa underlying the primary spongiosa was scanned and analyzed, starting 0.5 mm from the distal border of the epiphyseal plate. The threshold for bone was set at 446 mg HA/cm^3. Bone histomorphometric parameters were reported as described in the report of the American Society of Bone and Mineral Research Histomorphometry Nomenclature Committee (Parfitt et al. 1987). Trabecular bone parameters, including bone volume fraction (BV/TV), connectivity density (Conn.D.), trabecular number (Tb.N.), trabecular thickness (Tb.Th.), trabecular separation (Tb.Sp.), and volumetric bone mineral density (vBMD.), were quantified.

NanoCT

NanoCT was conducted with a GE Phoenix Nanotom-MTM instrument (GE Inspection Technologies; Lewiston, PA, USA). Explanted knee joints were secured in a sponge substrate within a 15 mL conical tube containing 70% ethanol fixation solution. The x-ray emission parameters for ~5 μm voxel resolution were 60 kV and 60 mA, and the number of acquired projections was 1,800. Sagittal and coronal slices were acquired and analyzed in a blinded fashion without the use of contrast. Data was collected and reconstruction performed with Phoenix datos2 software. 3D rendered volumes were subsequently analyzed with VG Studio Max (v 2.1; Heidelberg, Germany) software. To assess articular cartilage calcification, the tidemark was identified on MRI, and the cartilage thicknesses noted at fixed points in the cartilage-cartilage contact areas of both compartments. These dimensions were superimposed on corresponding nanoCT images, and the cartilage volume assessed for calcification.

Histology

After the multimodality radiographical analysis, the fixed legs were decalcified for 12 days using a formic acid solution (Immunocal; Decal Chemical Corp., Talman, NY, USA). Legs were then embedded in paraffin. Knees from each group were sectioned in the sagittal plane; care was taken to record the depth of the samples for precise co-location with the microMRI and nanoCT images. The sections were stained with haemotoxylin/eosin. Imaging of the sections was undertaken using a Axioplan 2 microscope with an AxioCam image capture system (Carl Zeiss AG, Oberkochen, Germany). Prepared sections (n = 3/group; two sections scored per individual and averaged) were scored using the Osteoarthritis Research Society International (OARSI) scoring system by a blinded cartilage expert (Gerwin et al. 2010). Briefly, the OARSI scoring is the standard protocol to assess cartilage erosion. The severity of cartilage degradation were characterized from micrographs and given a score of 0 (normal with no visible fibrillation or damage), 1 (minimal degradation), 2 (mild degradation), 3 (moderate degeneration), 4 (marked degradation), or 5 (severe degeneration with >75% of cartilage area damaged).

Statistics

Data were analyzed with a one-way ANOVA and a Tukey's post-hoc test to account for treatment effects using SigmaPlot version, 12.0 (Systat Software Inc., Richmond, CA, USA). For all tests, $P \leq 0.05$ was considered significant.

Results

Body Mass

Nine months postirradiation, the body masses were not significantly different (P>0.1) between unirradiated and irradiated rats: 0 Gy (493.7 g + 15.6), 1 Gy (485.7 g + 24.4), 3 Gy (447.3 g + 24.4), and 7 Gy (449.7 g + 25.3).

MRI

Nine months post-irradiation, the unirradiated rats had T2 values within the expected range for both the medial and lateral compartments of formalin-fixed tibial and femoral cartilage (Spandonis et al. 2004) and bovine nasal cartilage (Fishbein et al. 2007). T2 relaxation times in the tibial cartilage-cartilage contact areas of both the medial and lateral compartment were significantly shorter (P<0.05) in irradiated rats than in unirradiated rats at 9 months post-irradiation (Figure 2). Specifically, T2 relaxation times relative to the unirradiated controls (0 Gy) were decreased in the medial compartment: 1 Gy (-28.3%; P<0.01), 3 Gy (-23.1%; P<0.05), and 7 Gy (-15.7%; P<0.05), and in the lateral compartment: 1 Gy (-20.8%; P<0.05), 3 Gy (-23.1%; P=0.056), and 7 Gy (-28%; P<0.05).

T2 relaxation times in the femoral cartilage demonstrated increased variability than tibial cartilage for all groups (Figure 2). This was likely influenced by the technical difficulties in accurately identifying standing cartilage-cartilage contact areas. Although not statistically significant, reductions in T2 relaxation times were seen in the medial femoral condyle [1 Gy (-27.9%), 3 Gy (-26.5%), 7 Gy (-32.6%)] and in the lateral condyle [1 Gy (-36.7%), 3 Gy (-17.8%), 7 Gy (-38.4%)] compartments compared to the unirradiated controls.

MicroCT

Differences were observed in the microarchitectural properties of the trabecular bone that received 7 Gy relative to other groups (Table I). Conn.D. was significantly lower (P<0.05) in the 7 Gy rats than in the 1 Gy (-39%) and 3 Gy (-38%) rats, and marginally lower (P = 0.06) than in the unirradiated controls (-37%). Tb.N. was significantly lower (P<0.01) in the 7 Gy rats than in the unirradiated controls (-17%) and those that received 1 Gy (-20%) and 3 Gy (-19%) (Table I). Tb.Sp. was greater (P<0.001) in the 7 Gy rats than in the unirradiated control (+22%) and those that received 1 Gy (+27%) and 3 Gy (+26%).

NanoCT

Qualitative morphological assessment was performed on the rat knees following nanoCT imaging. None of the rats had evidence of peri-articular osteochondroma or other bone tumors. Trabecular bone changes were correctly identified, but not quantified in all of the irradiated rats. In the knee joint, peripheral osteophytes were observed in irradiated knees, but not in the unirradiated controls. Focus on the intra-articular soft tissues was limited to tissue calcification (Figure 3). Calcifications extending from the subchondral bone into the articular cartilage were observed; these have also been described in a rat osteoarthritis model (Roemhildt et al. 2012). Discrete intra-substance calcifications with no association to the subchondral bone were only observed in the irradiated cartilage (Figure 3). In addition, irradiated knees exhibited an increased incidence of ligament and capsular calcification.

Histology

Erosion of the cartilage lining the tibial plateau measured by the semi-quantitative OARSI scoring system identified mild to moderate cartilage degradation in the irradiated groups (Figure 4). At 0 Gy, the articular structure score was 1, indicating normal morphology without nicks or fibrillations. At 1 Gy, the score was 1.75, indicating minimal fibrillation. At 3 Gy, the score was 2, indicating a few nicks in the cartilage that run <25% of the thickness and some uplifting of articular cartilage from the underlying subchondral bone. At 7 Gy, the score was 4, indicating several nicks that run more than 50% the depth of the cartilage with some uplift of the articular cartilage from the subchondral bone.

Discussion

The underlying mechanism(s) responsible for the development of debilitating degenerative joint diseases in childhood cancer survivors is unclear. Imaging techniques such as microCT and histology have provided valuable insight into the extent and potential mechanism(s) of bone damage and fractures at irradiated sites using preclinical rodent models (Kondo et al. 2009; Wernle et al. 2010; Willey et al. 2010). However, this approach may not be sufficient to characterize the extent, progression, and mechanism(s) for joint damage after irradiation, as integrity of the joint relies on proper anatomy and molecular composition of both the hard (e.g. bone) and soft (e.g. articular cartilage) tissues that comprise the joint (Knecht et al. 2006; Fosang & Beier 2011; Loeser et al. 2012). We have incorporated advanced imaging approaches, qMRI and nanoCT, with more conventional approaches to assess long-term changes in whole-joint health in TBI rats. The rats were subjected to TBI doses while skeletal growth was ongoing and investigated after skeletal maturity at 9 months after irradiation, a period of ∼23 human years (Quinn 2005). Of note, we measured, i] long-term changes in T2 relaxation times in the articular cartilage of the weight-bearing regions of the knee joint (Dunn et al. 2004; Prasad et al. 2013; Wong et al. 2013), ii] intra-joint calcifications in the irradiated rats, iii] deficits in trabecular bone architecture which confirms results from microCT-based studies (Kondo et al. 2009; Alwood et al. 2010; Willey et al. 2010; Willey et al. 2011; Alwood et al. 2012; Green et al. 2012), and iv] some histologic evidence of cartilage erosion. Results from the novel imaging (qMRI and nanoCT) together with validated approaches (microCT and histology) were necessary to characterize the changes in the whole joint that could be suggestive of altered matrix molecular composition (Fishbein et al. 2007) or altered joint function (Fuerst et al. 2009; Kumar et al. 2013).

T2 qMRI sequencing holds promise as a translational measure of compositional and micro-architectural change in articular cartilage pathology. Its use is expanding to the clinic and pre-clinical animal models (Lupo et al. 2012; Olson et al. 2012; Bian et al. 2014). Discrete components of the T2 relaxation times relating to the cartilage zones have been reported with some variation using microMRI (Lattanzio et al. 2000; Reiter et al. 2009); however, the T2 relaxation times reported here refer to average overall transverse relaxation of the cartilage. The ROIs chosen for analysis were through the full thickness of the cartilage, normal to the surface, with equal representation of the constituent zones using a technique developed in our lab referred to as a “radiological biopsy” (Figure 1). This technique allows

us to individualize the contacting cartilage surfaces and eliminates the effects of partial voxel volume errors by only selecting voxels that are filled on contiguous 40 μm sections. This procedure allowed us to stay reproducibly within the articular cartilage throughout the signal decay; it was particularly important in our rat model, given the relatively exaggerated topography of a rat knee joint at the micro level.

Typically the T2 relaxation time is prolonged in osteoarthritic cartilage including juvenile idiopathic arthritis (Kim et al. 2010). This observation has been correlated with decreases in glycosaminoglycan content (Dunn et al. 2004; Prasad et al. 2013; Wong et al. 2013). Using a similar rodent model to the one presented here, Spandonis et al. (2004) investigated the effects of medial menisectomy, a biomechanical model of osteoarthritis, on T2 relaxation times from the formalin fixed knee cartilage of n = 4 Sprague Dawley rats. In the operated medial compartment that is subjected to mechanical cartilage degeneration in this model, they observed an increase in T2 relaxation times at 3 weeks after surgery. Thus, the decrease in the T2 relaxation times observed on the weight bearing cartilage-cartilage contact area of the tibial plateau of our irradiated rats was unexpected based on typical MRI biomarkers of cartilage degradation.

The significant decrease in T2 relaxation times (Figure 2) is suggestive of a radiation-specific pathological process leading to changes in cartilage composition in the weight bearing zones. Increased collagen-cross linking from irradiation is a potential cause for the lowered T2 relaxation times. Fixation of cartilage using 10% formalin has been shown to significantly lower T2 relaxation times versus unfixed controls (Fishbein et al. 2007); the observed reduction in T2 relaxation times in fixed versus unfixed samples was in-part attributed to increased cross-linking. Abnormal cross-linking of collagen has previously been reported as a late radiation effect in skeletal tissues, specifically bone (Gong et al. 2013; Tchanque-Fossuo et al. 2013). We present T2 relaxation times from the 0 Gy control group that are similar to those in the literature (Figure 2) (Spandonis et al. 2004). Therefore exposure to radiation may have affected cross-linking of the irradiated cartilage, accounting for the further decrease in T2 relaxation times vs. 0 Gy control. It should be noted that while elevated collagen cross-linking in cartilage is associated with increased stiffness of the structure (McGann et al. 2014), radiation has previously been shown to lower stiffness of articular cartilage after irradiation (Lindburg et al. 2013). Thus, both the status of collagen cross-links within the cartilage matrix and the biomechanical response of the tissue remain unclear. While tissue preparation techniques may impair our ability to interpret the absolute change in T2 relaxation times due to interactions between the fixed matrix and the matrix-bound/free water, the further lowering of T2 relaxation times versus controls with very low variance suggests radiation-induced changes in the matrix composition

Cartilage matrix formed from hypertrophic chondrocytes has also been shown to exhibit lower T2 relaxation times relative to that of mature chondrocytes (Potter et al. 2002). Hypertrophy of chondrocytes in the growth plate during skeletal development is a normal physiologic process that drives endochondral bone formation. This is in stark contrast to articular cartilage where hypertrophy of chondrocytes is a pathologic process associated with matrix calcification and arthritis (Gelse et al. 2012; Wei et al. 2012; Zhang et al. 2012; Nishida et al. 2013). Hypertrophic chondrocytes exhibit, i] reduced expression and

production of GAGs, ii] increased production of MMP-13 and collagen type X, and iii] increased production and activity of alkaline phosphatase (ALP) which facilitates calcification (Gelse et al. 2012; Wei et al. 2012; Zhang et al. 2012; Nishida et al. 2013). Hypertrophy of growth plate chondrocytes has been shown to occur after irradiation. This presumably contributes to the abnormal bone development and growth observed in childhood cancer survivors after treatment with radiation therapy (Damron et al. 2004b; Damron et al. 2004a; Margulies et al. 2006; Damron et al. 2008). Although radiation-induced hypertrophy of articular chondrocytes has not been characterized, several biomarkers of hypertrophy are elevated in human and pig articular chondrocytes after radiation exposure, including increased MMP-13 production and active degradation of GAGs (Willey et al. 2013). Moreover, a persistent increase in ALP activity and collagen type X expression from irradiated pig chondrocytes in 3-D culture has been published by our group in preliminary form (Willey & Lindburg 2014). Thus, persistent chondrocyte hypertrophy and the resultant alterations in the cartilage extracellular matrix represents a potential biologic mechanism for observed decrease in T2 relaxation times.

NanoCT imaging was incorporated in this model to assess chondrocalcinosis (i.e. calcification of the articular cartilage matrix); morphological assessment of the irradiated rat knee joints was performed concomitantly. The irradiated knees demonstrated discrete intra-substance calcifications in the articular cartilage (Figure 3). Intra-substance calcifications were distinguished from the more commonly encountered calcifications that arise directly from the subchondral bone (Roemhildt et al. 2012). No obvious peri-articular tumors, including osteochondromas, were detected in our irradiated rats.

Over the past decade, conventional microCT of irradiated bone has served as the basis for studies focused on characterizing the extent and cause of bone changes after clinical or spaceflight-relevant radiation exposures (Kondo et al. 2009; Alwood et al. 2010; Willey et al. 2010; Willey et al. 2011; Alwood et al. 2012; Green et al. 2012). In our model of radiation-induced joint damage, bone microarchitectural differences in the 7 Gy group (Table 1) were largely in agreement with other studies examining the radiation effects on the trabecular bone of rodents (Alwood et al. 2012; Green et al. 2012; Keenawinna et al. 2013), particularly when higher doses were used (Willey et al. 2008; Wernle et al. 2010). While biomechanical analyses were not performed, it is possible that this reduction in architectural parameters or perhaps altered bone matrix composition could compromise the strength of the joint and increase the risk of fracture (Wernle et al. 2010; Gong et al. 2013). Regardless, microCT analysis confirms long-term changes in trabecular bone after TBI in our rodent model.

A potential confounding factor that can lead to skeletal changes after exposure to radiation is that bone quantity and quality co-varies with body mass (Willey et al. 2008). However, relative to the unirradiated controls, the body mass of the irradiated rats decreased by <9%. Degradation of metaphyseal trabecular bone architecture was found at only the 7 Gy dose. Interestingly, the significant reduction in T2 relaxation times and the intra-joint calcifications after all radiation doses within the cartilage-cartilage contact areas do not appear to be associated with body mass. This finding likely relates to the long term follow-

up where the rats may have recovered systemically from the radiation exposure, but have residual joint damage as a direct result of the radiation exposure.

In conclusion, premature joint failure and decreased mobility are seen to be major sources of morbidity among adult survivors of childhood cancer. In this study, we demonstrate that TBI can induce clinically relevant degenerative changes in the articular cartilage of skeletally immature rats which can lead to late joint failure. This degenerative joint damage in rats can now be assessed using noninvasive imaging techniques that can be translated to the clinic. Thus, continued development these techniques using our skeletally immature rat model offers the opportunity to identify, i] prognostic indicators of joint degeneration in this "at risk" population, and ii] targets for prophylactic and therapeutic biological strategies to prevent or ameliorate long term joint damage in the survivors of childhood cancer.

Acknowledgments

We would like to gratefully acknowledge Dr. Michael Robbins for his mentoring, training, and enthusiasm for pursuing research in the field of late radiation-induced skeletal injury. Dr. Ted Bateman graciously provided access to the microCT. We thank Dr. Raghunatha Yammani for scoring all the histologic slides for cartilage damage. This work was supported in part by a National Space Biomedical Research Institute Career Advancement Award EO00008 through NASA NCC 9-58 [JSW], R01-CA136910-S1 [MTM], R01-CA112593-S1 to Michael E Robbins, the Physician Scientist Training Program in Orthopaedic Surgery [L.A. Koman, MD] and National Science Foundation Award # 0959511 [BC].

References

Alwood JS, Kumar A, Tran LH, Wang A, Limoli CL, Globus RK. Low-dose, ionizing radiation and age-related changes in skeletal microarchitecture. J Aging Res. 2012; 2012:481983. [PubMed: 22570786]

Alwood JS, Yumoto K, Mojarrab R, Limoli CL, Almeida EA, Searby ND, Globus RK. Heavy ion irradiation and unloading effects on mouse lumbar vertebral microarchitecture, mechanical properties and tissue stresses. Bone. 2010; 47(2):248–55. [PubMed: 20466089]

Andreisek G, Weiger M. T2* mapping of articular cartilage: current status of research and first clinical applications. Invest Radiol. 2014; 49(1):57–62. [PubMed: 24056113]

Armenian SH, Sun CL, Kawashima T, Arora M, Leisenring W, Sklar CA, Baker KS, Francisco L, Teh JB, Mills G, et al. Long-term health-related outcomes in survivors of childhood cancer treated with HSCT versus conventional therapy: a report from the Bone Marrow Transplant Survivor Study (BMTSS) and Childhood Cancer Survivor Study (CCSS). Blood. 2011; 118(5):1413–20. [PubMed: 21652685]

Bhatia S, Sklar C. Second cancers in survivors of childhood cancer. Nat Rev Cancer. 2002; 2(2):124–32. [PubMed: 12635175]

Bian W, Hess CP, Chang SM, Nelson SJ, Lupo JM. Susceptibility-weighted MR imaging of radiation therapy-induced cerebral microbleeds in patients with glioma: a comparison between 3T and 7T. Neuroradiology. 2014; 56(2):91–6. [PubMed: 24281386]

Braam KI, van der Torre P, Takken T, Veening MA, van Dulmen-den Broeder E, Kaspers GJ. Physical exercise training interventions for children and young adults during and after treatment for childhood cancer. Cochrane Database Syst Rev. 2013; 4:CD008796. [PubMed: 23633361]

Bullough PG, DiCarlo EF. Subchondral avascular necrosis: a common cause of arthritis. Ann Rheum Dis. 1990; 49(6):412–20. [PubMed: 2200357]

Chemaitilly W, Boulad F, Heller G, Kernan NA, Small TN, O'Reilly RJ, Sklar CA. Final height in pediatric patients after hyperfractionated total body irradiation and stem cell transplantation. Bone Marrow Transplant. 2007; 40(1):29–35. [PubMed: 17468769]

Collis CH, Dieppe PA, Bullimore JA. Radiation-induced chondrocalcinosis of the knee articular cartilage. Clin Radiol. 1988; 39(4):450–1. [PubMed: 3180660]

Cornelissen M, de Ridder L. Dose- and time-dependent increase of lysosomal enzymes in embryonic cartilage in vitro after ionizing radiation. Scanning Microsc. 1990; 4(3):769–73. discussion 773-4. [PubMed: 1706891]

Cornelissen M, Thierens H, de Ridder L. Effects of ionizing radiation on the size distribution of proteoglycan aggregates synthesized by chondrocytes in agarose. Scanning Microsc. 1993; 7(4): 1263–7. discussion 1267-8. [PubMed: 8023093]

Cornelissen M, Thierens H, De Ridder L. Effects of ionizing radiation on cartilage: emphasis on effects on the extracellular matrix. Scanning Microsc. 1996; 10(3):833–40. [PubMed: 9813643]

Damron TA, Mathur S, Horton JA, Strauss J, Margulies B, Grant W, Farnum CE, Spadaro JA. Temporal changes in PTHrP, Bcl-2, Bax, caspase, TGF-beta, and FGF-2 expression following growth plate irradiation with or without radioprotectant. J Histochem Cytochem. 2004a; 52(2): 157–67. [PubMed: 14729867]

Damron TA, Horton JA, Naqvi A, Margulies B, Strauss J, Grant W, Farnum CE, Spadaro JA. Decreased proliferation precedes growth factor changes after physeal irradiation. Clin Orthop Relat Res. 2004b; (422):233–42. [PubMed: 15187862]

Damron TA, Horton JA, Pritchard MR, Stringer MT, Margulies BS, Strauss JA, Spadaro JA, Farnum CE. Histomorphometric evidence of growth plate recovery potential after fractionated radiotherapy: an in vivo model. Radiat Res. 2008; 170(3):284–91. [PubMed: 18763859]

Damron TA, Zhang M, Pritchard MR, Middleton FA, Horton JA, Margulies BM, Strauss JA, Farnum CE, Spadaro JA. Microarray cluster analysis of irradiated growth plate zones following laser microdissection. Int J Radiat Oncol Biol Phys. 2009; 74(3):949–56. [PubMed: 19480974]

Dunn TC, Lu Y, Jin H, Ries MD, Majumdar S. T2 relaxation time of cartilage at MR imaging: comparison with severity of knee osteoarthritis. Radiology. 2004; 232(2):592–8. [PubMed: 15215540]

Faraci M, Barra S, Cohen A, Lanino E, Grisolia F, Miano M, Foppiano F, Sacco O, Cabria M, De Marco R, et al. Very late nonfatal consequences of fractionated TBI in children undergoing bone marrow transplant. Int J Radiat Oncol Biol Phys. 2005; 63(5):1568–75. [PubMed: 15990246]

Fishbein KW, Gluzband YA, Kaku M, Ambia-Sobhan H, Shapses SA, Yamauchi M, Spencer RG. Effects of formalin fixation and collagen cross-linking on T2 and magnetization transfer in bovine nasal cartilage. Magn Reson Med. 2007; 57(6):1000–11. [PubMed: 17534923]

Fletcher BD, Crom DB, Krance RA, Kun LE. Radiation-induced bone abnormalities after bone marrow transplantation for childhood leukemia. Radiology. 1994; 191(1):231–5. [PubMed: 8134578]

Fosang AJ, Beier F. Emerging Frontiers in cartilage and chondrocyte biology. Best Pract Res Clin Rheumatol. 2011; 25(6):751–66. [PubMed: 22265258]

Fuerst M, Bertrand J, Lammers L, Dreier R, Echtermeyer F, Nitschke Y, Rutsch F, Schafer FK, Niggemeyer O, Steinhagen J, et al. Calcification of articular cartilage in human osteoarthritis. Arthritis Rheum. 2009; 60(9):2694–703. [PubMed: 19714647]

Gelse K, Ekici AB, Cipa F, Swoboda B, Carl HD, Olk A, Hennig FF, Klinger P. Molecular differentiation between osteophytic and articular cartilage--clues for a transient and permanent chondrocyte phenotype. Osteoarthritis Cartilage. 2012; 20(2):162–71. [PubMed: 22209871]

Gerwin N, Bendele AM, Glasson S, Carlson CS. The OARSI histopathology initiative - recommendations for histological assessments of osteoarthritis in the rat. Osteoarthritis Cartilage. 2010; 18(Suppl 3):S24–34. [PubMed: 20864021]

Gong B, Oest ME, Mann KA, Damron TA, Morris MD. Raman spectroscopy demonstrates prolonged alteration of bone chemical composition following extremity localized irradiation. Bone. 2013; 57(1):252–8. [PubMed: 23978492]

Green DE, Adler BJ, Chan ME, Rubin CT. Devastation of adult stem cell pools by irradiation precedes collapse of trabecular bone quality and quantity. J Bone Miner Res. 2012; 27(4):749–59. [PubMed: 22190044]

Greene-Schloesser D, Robbins ME, Peiffer AM, Shaw EG, Wheeler KT, Chan MD. Radiation-induced brain injury: A review. Front Oncol. 2012; 2:73. [PubMed: 22833841]

Hansson LI, Menander-Sellman K, Stenstrom A, Thorngren KG. Rate of normal longitudinal bone growth in the rat. Calcif Tissue Res. 1972; 10(3):238–51. [PubMed: 4639288]

Henkelman RM, Stanisz GJ, Kim JK, Bronskill MJ. Anisotropy of NMR properties of tissues. Magn Reson Med. 1994; 32(5):592–601. [PubMed: 7808260]

Hudson MM, Mertens AC, Yasui Y, Hobbie W, Chen H, Gurney JG, Yeazel M, Recklitis CJ, Marina N, Robison LR, et al. Health status of adult long-term survivors of childhood cancer: a report from the Childhood Cancer Survivor Study. JAMA. 2003; 290(12):1583–92. [PubMed: 14506117]

Kaste SC, Shidler TJ, Tong X, Srivastava DK, Rochester R, Hudson MM, Shearer PD, Hale GA. Bone mineral density and osteonecrosis in survivors of childhood allogeneic bone marrow transplantation. Bone Marrow Transplant. 2004; 33(4):435–41. [PubMed: 14716354]

Kazakia GJ, Kuo D, Schooler J, Siddiqui S, Shanbhag S, Bernstein G, Horvai A, Majumdar S, Ries M, Li X. Bone and cartilage demonstrate changes localized to bone marrow edema-like lesions within osteoarthritic knees. Osteoarthritis Cartilage. 2013; 21(1):94–101. [PubMed: 23025926]

Keenawinna L, Oest ME, Mann KA, Spadaro J, Damron TA. Zoledronic acid prevents loss of trabecular bone after focal irradiation in mice. Radiat Res. 2013; 180(1):89–99. [PubMed: 23772924]

Kerckhofs G, Sainz J, Wevers M, Van de Putte T, Schrooten J. Contrast-enhanced nanofocus computed tomography images the cartilage subtissue architecture in three dimensions. Eur Cell Mater. 2013; 25:179–89. [PubMed: 23389752]

Kim HK, Laor T, Graham TB, Anton CG, Salisbury SR, Racadio JM, Dardzinski BJ. T2 relaxation time changes in distal femoral articular cartilage in children with juvenile idiopathic arthritis: a 3-year longitudinal study. AJR Am J Roentgenol. 2010; 195(4):1021–5. [PubMed: 20858834]

King EA, Hanauer DA, Choi SW, Jong N, Hamstra DA, Li Y, Farley FA, Caird MS. Osteochondromas After Radiation for Pediatric Malignancies: A Role for Expanded Counseling for Skeletal Side Effects. J Pediatr Orthop. 2013

Knecht S, Vanwanseele B, Stussi E. A review on the mechanical quality of articular cartilage - implications for the diagnosis of osteoarthritis. Clin Biomech (Bristol, Avon). 2006; 21(10):999–1012.

Kobos R, Steinherz PG, Kernan NA, Prockop SE, Scaradavou A, Small TN, Shukla N, Khalaf R, O'Reilly RJ, Boulad F. Allogeneic hematopoietic stem cell transplantation for pediatric patients with treatment-related myelodysplastic syndrome or acute myelogenous leukemia. Biol Blood Marrow Transplant. 2012; 18(3):473–80. [PubMed: 22079789]

Kolar J, Vrabec R, Chyba J. Arthropathies after irradiation. J Bone Joint Surg Am. 1967; 49(6):1157–66. [PubMed: 6038861]

Kondo H, Searby ND, Mojarrab R, Phillips J, Alwood J, Yumoto K, Almeida EA, Limoli CL, Globus RK. Total-body irradiation of postpubertal mice with (137)Cs acutely compromises the microarchitecture of cancellous bone and increases osteoclasts. Radiat Res. 2009; 171(3):283–9. [PubMed: 19267555]

Kumar D, Subburaj K, Lin W, Karampinos DC, McCulloch CE, Li X, Link TM, Souza RB, Majumdar S. Quadriceps and hamstrings morphology is related to walking mechanics and knee cartilage MRI relaxation times in young adults. The Journal of orthopaedic and sports physical therapy. 2013; 43(12):881–90. [PubMed: 24175607]

Lammentausta E, Kiviranta P, Nissi MJ, Laasanen MS, Kiviranta I, Nieminen MT, Jurvelin JS. T2 relaxation time and delayed gadolinium-enhanced MRI of cartilage (dGEMRIC) of human patellar cartilage at 1.5 T and 9.4 T: Relationships with tissue mechanical properties. J Orthop Res. 2006; 24(3):366–74. [PubMed: 16479569]

Lattanzio PJ, Marshall KW, Damyanovich AZ, Peemoeller H. Macromolecule and water magnetization exchange modeling in articular cartilage. Magn Reson Med. 2000; 44(6):840–51. [PubMed: 11108620]

Leiper AD, Stanhope R, Lau T, Grant DB, Blacklock H, Chessells JM, Plowman PN. The effect of total body irradiation and bone marrow transplantation during childhood and adolescence on growth and endocrine function. Br J Haematol. 1987; 67(4):419–26. [PubMed: 3322361]

Lindburg CA, Willey JS, Dean D. Effects of low dose X-ray irradiation on porcine articular cartilage explants. J Orthop Res. 2013; 31(11):1780–5. [PubMed: 23913833]

Loeser RF, Goldring SR, Scanzello CR, Goldring MB. Osteoarthritis: a disease of the joint as an organ. Arthritis Rheum. 2012; 64(6):1697–707. [PubMed: 22392533]

Lupo JM, Chuang CF, Chang SM, Barani IJ, Jimenez B, Hess CP, Nelson SJ. 7-Tesla susceptibility-weighted imaging to assess the effects of radiotherapy on normal-appearing brain in patients with glioma. Int J Radiat Oncol Biol Phys. 2012; 82(3):e493–500. [PubMed: 22000750]

Margulies BS, Horton JA, Wang Y, Damron TA, Allen MJ. Effects of radiation therapy on chondrocytes in vitro. Calcif Tissue Int. 2006; 78(5):302–13. [PubMed: 16691495]

McGann ME, Bonitsky CM, Ovaert TC, Wagner DR. The effect of collagen crosslinking on the biphasic poroviscoelastic cartilage properties determined from a semi-automated microindentation protocol for stress relaxation. J Mech Behav Biomed Mater. 2014; 34C:264–272. [PubMed: 24631625]

Miyazaki O, Nishimura G, Okamoto R, Masaki H, Kumagai M, Shioda Y, Nozawa K, Kitoh H. Induction of systemic bone changes by preconditioning total body irradiation for bone marrow transplantation. Pediatr Radiol. 2009; 39(1):23–9. [PubMed: 18953533]

Mostoufi-Moab S, Ginsberg JP, Bunin N, Zemel B, Shults J, Leonard MB. Bone density and structure in long-term survivors of pediatric allogeneic hematopoietic stem cell transplantation. J Bone Miner Res. 2012; 27(4):760–9. [PubMed: 22189761]

Mostoufi-Moab S, Isaacoff EJ, Spiegel D, Gruccio D, Ginsberg JP, Hobbie W, Shults J, Leonard MB. Childhood cancer survivors exposed to total body irradiation are at significant risk for slipped capital femoral epiphysis during recombinant growth hormone therapy. Pediatr Blood Cancer. 2013; 60(11):1766–71. [PubMed: 23818448]

Nishida T, Kubota S, Aoyama E, Takigawa M. Impaired glycolytic metabolism causes chondrocyte hypertrophy-like changes via promotion of phospho-Smad1/5/8 translocation into nucleus. Osteoarthritis Cartilage. 2013; 21(5):700–9. [PubMed: 23384547]

Oeffinger KC, Bhatia S. Second primary cancers in survivors of childhood cancer. Lancet. 2009; 374(9700):1484–5. [PubMed: 19880005]

Oeffinger KC, Mertens AC, Sklar CA, Kawashima T, Hudson MM, Meadows AT, Friedman DL, Marina N, Hobbie W, Kadan-Lottick NS, et al. Chronic health conditions in adult survivors of childhood cancer. N Engl J Med. 2006; 355(15):1572–82. [PubMed: 17035650]

Olson JD, Walb MC, Moore JE, Attia A, Sawyer HL, McBride JE, Wheeler KT, Miller MS, Munley MT. A gated-7T MRI technique for tracking lung tumor development and progression in mice after exposure to low doses of ionizing radiation. Radiat Res. 2012; 178(4):321–7. [PubMed: 22950352]

Parfitt AM, Drezner MK, Glorieux FH, Kanis JA, Malluche H, Meunier PJ, Ott SM, Recker RR. Bone histomorphometry: standardization of nomenclature, symbols, and units. Report of the ASBMR Histomorphometry Nomenclature Committee. J Bone Miner Res. 1987; 2(6):595–610. [PubMed: 3455637]

Potter K, Leapman RD, Basser PJ, Landis WJ. Cartilage calcification studied by proton nuclear magnetic resonance microscopy. J Bone Miner Res. 2002; 17(4):652–60. [PubMed: 11918222]

Prasad AP, Nardo L, Schooler J, Joseph GB, Link TM. T(1)rho and T(2) relaxation times predict progression of knee osteoarthritis. Osteoarthritis Cartilage. 2013; 21(1):69–76. [PubMed: 23059757]

Pritchard MR, Horton JA, Keenawinna LS, Damron TA. Microarray analysis of irradiated growth plate zones following laser microdissection shows later importance of differentially expressed genes during radiorecovery. Cells Tissues Organs. 2010; 192(4):240–9. [PubMed: 20616531]

Quinn R. Comparing rat's to human's age: how old is my rat in people years? Nutrition. 2005; 21(6): 775–7. [PubMed: 15925305]

Raya JG, Dietrich O, Horng A, Weber J, Reiser MF, Glaser C. T2 measurement in articular cartilage: impact of the fitting method on accuracy and precision at low SNR. Magn Reson Med. 2010; 63(1):181–93. [PubMed: 19859960]

Recht MP, Goodwin DW, Winalski CS, White LM. MRI of articular cartilage: revisiting current status and future directions. AJR Am J Roentgenol. 2005; 185(4):899–914. [PubMed: 16177408]

Reiter DA, Lin PC, Fishbein KW, Spencer RG. Multicomponent T2 relaxation analysis in cartilage. Magn Reson Med. 2009; 61(4):803–9. [PubMed: 19189393]

Roemhildt ML, Beynnon BD, Gardner-Morse M. Mineralization of articular cartilage in the Sprague-Dawley rat: characterization and mechanical analysis. Osteoarthritis Cartilage. 2012; 20(7):796–800. [PubMed: 22531460]

Rueegg CS, Gianinazzi ME, Rischewski J, Beck Popovic M, von der Weid NX, Michel G, Kuehni CE. Health-related quality of life in survivors of childhood cancer: the role of chronic health problems. J Cancer Surviv. 2013

Shido Y, Maeda N, Kato K, Horibe K, Tsukushi S, Ishiguro N, Nishida Y. Osteochondroma with metaphyseal abnormalities after total body irradiation followed by stem cell transplantation. J Pediatr Hematol Oncol. 2012; 34(5):378–82. [PubMed: 22246151]

Spandonis Y, Heese FP, Hall LD. High resolution MRI relaxation measurements of water in the articular cartilage of the meniscectomized rat knee at 4.7 T. Magn Reson Imaging. 2004; 22(7): 943–51. [PubMed: 15288135]

Stone AV, Loeser RF, Vanderman KS, Long DL, Clark SC, Ferguson CM. Pro-inflammatory stimulation of meniscus cells increases production of matrix metalloproteinases and additional catabolic factors involved in osteoarthritis pathogenesis. Osteoarthritis Cartilage. 2014; 22(2):264–74. [PubMed: 24315792]

Tchanque-Fossuo CN, Gong B, Poushanchi B, Donneys A, Sarhaddi D, Gallagher KK, Deshpande SS, Goldstein SA, Morris MD, Buchman SR. Raman spectroscopy demonstrates Amifostine induced preservation of bone mineralization patterns in the irradiated murine mandible. Bone. 2013; 52(2): 712–7. [PubMed: 22885239]

Tremoleda JL, Khalil M, Gompels LL, Wylezinska-Arridge M, Vincent T, Gsell W. Imaging technologies for preclinical models of bone and joint disorders. EJNMMI Res. 2011; 1(1):11. [PubMed: 22214535]

Walb MC, Moore JE, Attia A, Wheeler KT, Miller MS, Munley MT. A technique for murine irradiation in a controlled gas environment. Biomed Sci Instrum. 2012; 48:470–7. [PubMed: 22846321]

Walker PS, Yildirim G, Sussman-Fort J, Klein GR. Relative positions of the contacts on the cartilage surfaces of the knee joint. Knee. 2006; 13(5):382–8. [PubMed: 16790353]

Wei F, Zhou J, Wei X, Zhang J, Fleming BC, Terek R, Pei M, Chen Q, Liu T, Wei L. Activation of Indian hedgehog promotes chondrocyte hypertrophy and upregulation of MMP-13 in human osteoarthritic cartilage. Osteoarthritis Cartilage. 2012; 20(7):755–63. [PubMed: 22469853]

Wernle JD, Damron TA, Allen MJ, Mann KA. Local irradiation alters bone morphology and increases bone fragility in a mouse model. J Biomech. 2010; 43(14):2738–46. [PubMed: 20655052]

Willey JS, Lindburg CA. Radiation increases biomarkers for hypertrophy in articular chondrocytes. Orthopaedic Research Society Annual Meeting. 2014:63.

Willey JS, Lloyd SA, Nelson GA, Bateman TA. Ionizing radiation and bone loss: space exploration and clinical therapy applications. Clinical Reviews: Bone and Mineral Metabolism. 2011; 9:54–62.

Willey JS, Long DL, Vanderman KS, Loeser RF. Ionizing radiation causes active degradation and reduces matrix synthesis in articular cartilage. Int J Radiat Biol. 2013; 89(4):268–77. [PubMed: 23134087]

Willey JS, Livingston EW, Robbins ME, Bourland JD, Tirado-Lee L, Smith-Sielicki H, Bateman TA. Risedronate prevents early radiation-induced osteoporosis in mice at multiple skeletal locations. Bone. 2010; 46(1):101–11. [PubMed: 19747571]

Willey JS, Grilly LG, Howard SH, Pecaut MJ, Obenaus A, Gridley DS, Nelson GA, Bateman TA. Bone architectural and structural properties after 56Fe26+ radiation-induced changes in body mass. Radiat Res. 2008; 170(2):201–7. [PubMed: 18666808]

Wong CS, Yan CH, Gong NJ, Li T, Chan Q, Chu YC. Imaging biomarker with T1rho and T2 mappings in osteoarthritis - in vivo human articular cartilage study. Eur J Radiol. 2013; 82(4):647–50. [PubMed: 23333531]

Zhang W, Chen J, Zhang S, Ouyang HW. Inhibitory function of parathyroid hormone-related protein on chondrocyte hypertrophy: the implication for articular cartilage repair. Arthritis Res Ther. 2012; 14(4):221. [PubMed: 22971952]

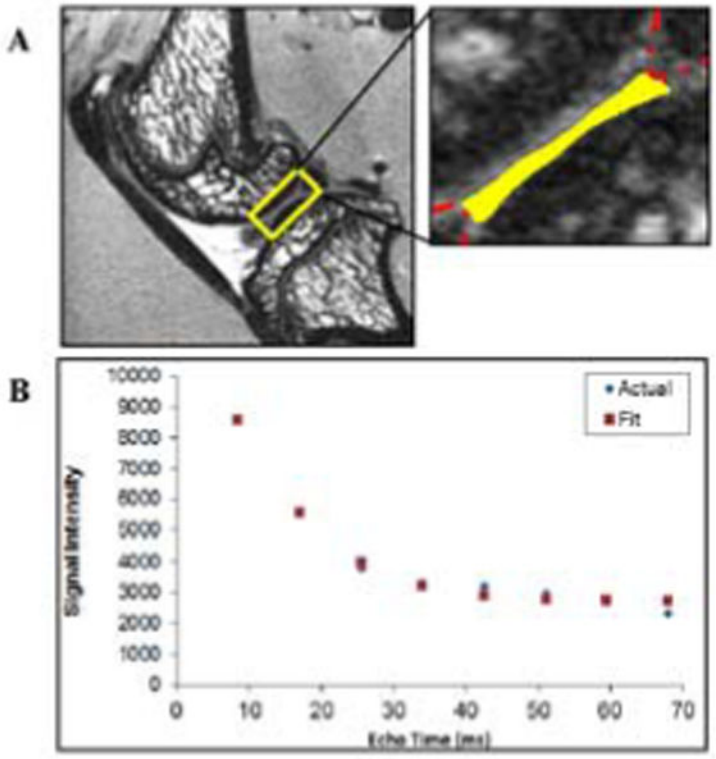

Figure 1.

A T2 weighted sagittal image of the center of the lateral compartment of a rat knee joint. (**A**) A typical region of interest from which T2 relaxation data were assessed is outlined with the solid line.. In this case, the cartilage-cartilage contact area lining the tibial plateau is highlighted. The anterior and posterior aspects of the lateral meniscus are outlined with the broken line. (**B**) A representative curve fit plot showing the mean signal intensity of the 40 μm voxels in the ROI and the points on a best fit noise corrected exponential decay curve. This particular specimen had a T2 of 16.4 ms, (R^2 = 0.99).

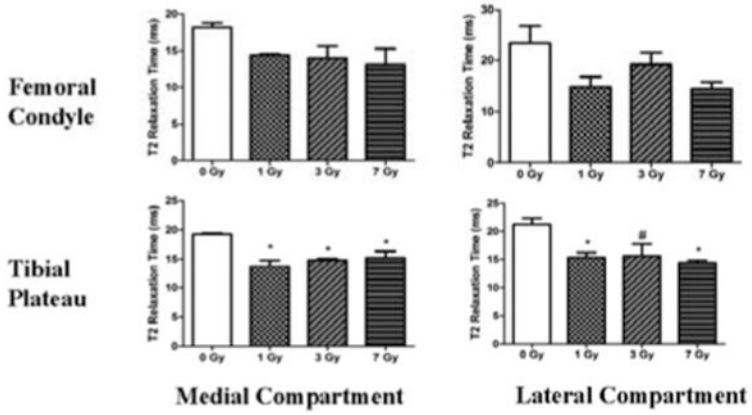

Figure 2.

T2 relaxation times from the cartilage-cartilage contact areas lining the tibial plateau and femoral condyles of adult rats at 9 months after TBI. The T2 relaxation times are presented for the weight-bearing cartilage-cartilage contact areas from the medial (left) and lateral (right) compartments of the femoral condyles (top) and tibial plateaus (bottom). Error bars represent SEM. The asterisks (*) indicates a significant difference ($P < 0.05$) compared to 0 Gy controls using a one-way ANOVA and Tukey Post Hoc Test. The hash (#) indicates a marginally significant difference ($P=0.056$) compared to 0 Gy controls. All other data were not significantly different from the 0 Gy controls, although the P-values were < 0.1.

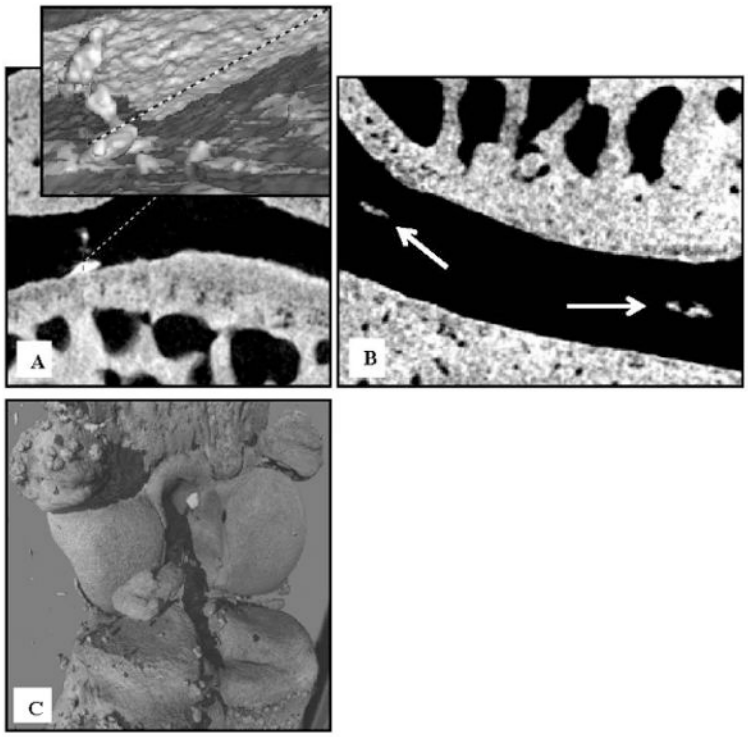

Figure 3.

Representative nanoCT images of an irradiated rat knee at 9 months after TBI. **A**) Calcifications extending from the subchondral bone into the articular cartilage of a 3 Gy rat identified on a topographic reconstruction of the interface of bone and the calcified cartilage layer. **B**) Coronal view of discrete intra-substance calcifications in a 7 Gy rat knee. **C**) Extensive calcification of the capsule and intra-articular structures is shown on a 3-D reconstructed view of a 3 Gy rat knee.

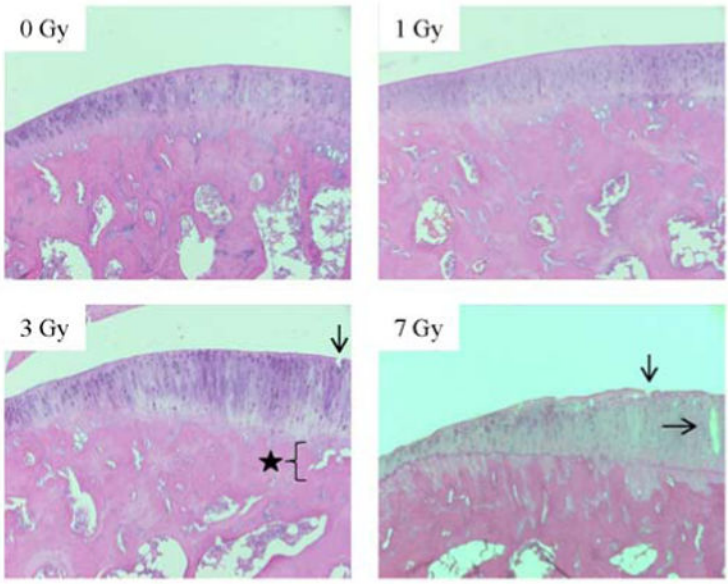

Figure 4.

Representative histology images (100X magnification) of the articular cartilage lining the medial tibial plateau of rats. The images are all taken from the articular cartilage underlying the posterior meniscal horn of the medial condyle. Black arrows indicate defects that extend down into the articular cartilage. The star indicates a discrete location of articular cartilage uplifting from the subchondral bone at the tidemark.

Table I

Parameters of trabecular architecture and density in the metaphyseal bone of the proximal tibiae in rats at 1 year after irradiation.

	0 Gy			1 Gy			3 Gy			7 Gy		
	LSM		**SD**	**LSM**		**SD**	**LSM**		**SD**	**LSM**		**SD**
BV/TV (%)	15.2	±	2.7	13.5	±	2.8	14.8	±	3.0	10.2	±	1.7
Conn.Dens. (1/mm^3)	31.5	±	7.3	35.1	±	7.2	34.6	±	7.5	21.4	±	4.2 *b,c*
Tb.Th (μm)	80	±	3	75	±	5	78	±	6	76	±	5
Tb.N. (1/mm^3)	2.85	±	0.27	2.97	±	0.16	2.92	±	0.22	2.36	±	0.13 *a,B,C*
Tb.Sp (μm)	339	±	38	328	±	21	331	±	28	417	±	26 *A,B,C*
vBMD	185.4	±	30.0	182.5	±	37.0	180.4	±	19.7	143.6	±	27.9

Note: All values presented as least squares mean ± SD using a one-way ANOVA with Tukey post hoc tests. Lowercase letters indicate significance at $P < 0.05$ vs.

a control;

b 1 Gy; and

c 3 Gy.

Uppercase letters indicate significance at $P < 0.01$ vs.

A control;

B 1 Gy; and

C 3 Gy.